

Numerical Analysis of Quantum Speed Limits: controlled quantum spin chain systems with constrained control functions

Benjamin Russell, Susan Stepney

Department of Computer Science, University of York, UK, YO10 5DD
bjr502@york.ac.uk, susan.stepney@york.ac.uk

Abstract. We are interested in fundamental limits to computation imposed by physical constraints. In particular, the physical laws of motion constrain the speed at which a computer can transition between well-defined states. Certain time bounds are known, but these are not tight bounds. For computation, we also need to consider bounds in the presence of control functions. Here, we use a numerical search approach to discover specific optimal control schemes. We present results for two coupled spins controlled in two scenarios: (i) a single control field influencing each spin separately; (ii) two orthogonal control fields influencing each spin.

1 Introduction

Computers operate under physical laws, which constrain their operation. In particular, the physical laws of motion constrain the speed at which a computer can transition between well-defined states.

In the case of quantum systems, certain fundamental bounds on these transition times are known. The Margolus-Levitin bound [5] demonstrates the limit to the speed of dynamical evolution of any quantum system with a time-independent Hamiltonian as imposed by the energy expectation. This and other such speed limit bounds have an interpretation in terms of the maximum information processing rate of a quantum systems [4]. This bound complements the Mandelstam-Tamm inequality [12], a bound to the speed of dynamical evolution of a quantum system in terms of the energy *uncertainty*.

When considering a quantum computer, we consider a system A implementing a computation and a system B producing the control fields specifying the particular computation. Together these can be considered to be subsystems of a larger quantum system $A \otimes B$. This highlights that the control functions are implemented by some quantum system, and the limits quantum mechanics places on the dynamics of the system producing the control fields places limits on the control fields themselves. Hence, as well as the computational system A , the control functions B are also subject to physical constraints.

These constraints arise variously. The energy available for the production of control fields limits is one obvious restriction. However there are other limitations that arise from physical constraints, presented by physical laws rather than

engineering difficulties or limitations on resources, on the devices producing the control fields. For example, allowing more energy to produce the control fields could allow the production of fields with greater amplitudes, however, no amount of energy could facilitate any part of the device producing control fields to move faster than the vacuum speed of light; this can constrain the frequency of time-varying fields. Ultimately the device producing the control fields is subject to the laws of quantum mechanics and relativity, which limit the detail with which a control field can be specified, and the rate at which it can change in time.

As a consequence, when attempting to understand the physical limits to the speed of quantum computers, we must also take into account the limits placed on computation speed by constraints on the control functions.

First we introduce an exemplar problem and certain plausible constraints (§2). Next we describe the optimisation problem approach (§3). Then we describe the numerical approach we use for finding optimal solutions (§4). We then apply this approach to a two-bit chain, deriving specific results (§5).

2 The Exemplar Problem

2.1 Heisenberg spin chain

To investigate the effect of constraints on the control function, we consider an exemplar problem relevant to quantum computation: a controlled Heisenberg spin chain of N spins (with coupling constants J_x, J_y, J_z . This has Hamiltonian [6]:

$$\begin{aligned} & \sum_{k \in \{x,y,z\}} J_k \left(\sum_{n=0}^{N-2} \hat{I}_2^{\otimes n} \otimes \sigma^k \otimes \sigma^k \otimes \hat{I}_2^{\otimes N-n-2} \right) \\ & + \sum_{n=0}^{N-1} g_n(t) \hat{I}_2^{\otimes n} \otimes \sigma^z \otimes \hat{I}_2^{\otimes N-n-1} \\ & + \sum_{n=0}^{N-1} h_n(t) \hat{I}_2^{\otimes n} \otimes \sigma^y \otimes \hat{I}_2^{\otimes N-n-1} \end{aligned} \quad (1)$$

where: σ^k is the k^{th} standard Pauli matrix; the g_n and h_n represent the externally generated, potentially time-dependant, control fields in the z and y directions respectively. For the case of a single, z direction, control field per spin, the h_n are zero.

Two central problems in quantum optimal control are: 1) Determine whether or not a specific system can implement a desired unitary time evolution (control-ability); and, if so, 2) how quickly this desired transformation can be achieved (time optimality) [11]. It is the second of these, specifically for a Heisenberg model spin chain, that we address here.

2.2 Band-Limited Fourier Series For Representing Control Functions with Bounded Rate of Change

In [8] we study geometric methods for determining speed limits on implementing quantum information processing tasks in the presence of constraints of the control functions of a constrained quantum system. There, no comment is made about constraints on the *time derivatives* of the control functions. Such constraints represent the maximum rate at which a control function can change. Here, we have chosen to represent control functions $g_k(t)$ ($t \in [0, \tau]$, $\tau \leq 1$) which have bounded rate of change by band-limited Fourier series:

$$g_k(t) = \frac{a_{k,0}}{2} + \sum_{m=1}^M (a_{k,m} \sin(mt) + b_{k,m} \cos(mt)) \quad (2)$$

where the relationship between the Fourier coefficients $\{a_{k,m}, b_{k,m}\}$ and the control function g_k are given by the usual formula. (For simplicity in the following discussions we ignore the orthogonal control field h_k ; they are either treated analogously to the g_k in the two control field case, or are zero in the one control field case.)

We can easily find a bound on the magnitude of the derivative of each control function g_k in terms of its degree of band-limiting M and its largest Fourier coefficient $A_k = \max\{|a_{k,m}|, |b_{k,m}|\}$:

$$\left| \frac{d}{dt} g_k(t) \right|^2 = \left| \frac{d}{dt} \sum_{m=1}^M (a_{k,m} \sin(mt) + b_{k,m} \cos(mt)) \right|^2 \quad (3)$$

$$= \left| \sum_{m=1}^M m (a_{k,m} \cos(mt) - b_{k,m} \sin(mt)) \right|^2 \quad (4)$$

$$\leq \sum_{m=1}^M m^2 |a_{k,m} \cos(mt) - b_{k,m} \sin(mt)|^2 \quad (5)$$

$$\leq \sum_{m=1}^M m^2 (a_{k,m}^2 \cos^2(mt) - a_{k,m} b_{k,m} \sin(2mt) + b_{k,m}^2 \sin^2(mt)) \quad (6)$$

$$\leq \sum_{m=1}^M m^2 (a_{k,m}^2 + b_{k,m}^2 + 1) \quad (7)$$

$$\leq (2A_k + 1) \sum_{m=1}^M m^2 = (2A_k + 1)M(M+1)(2M+1)/6 \quad (8)$$

2.3 Band-Limited Fourier Series For Representing Control Functions with Bounded Power

In this band-limited Fourier representation, the constraint that the total energy used to produce each of the control fields individually (the power) is bounded

by κ takes a simple form due to Parseval's theorem. The desired constraint is:

$$\int_0^\tau g_k^2(t)dt \leq \kappa^2 \quad (9)$$

which represents the constraint on the total power used in the production of the control fields. Parseval's theorem tell us that:

$$\int_0^\tau g_k^2(t)dt = \frac{1}{\tau} \sum_{m=0}^M (a_{k,m}^2 + b_{k,m}^2) \quad (10)$$

3 Optimisation problem

3.1 General optimisation

We wish to find control functions which maximise functionals (whose relevance is described in [1] and elsewhere) of the form:

$$F[\mathbf{g}] = \Re \text{Tr}(\hat{O}^\dagger \hat{U}_t) \quad (11)$$

where \mathbf{g} is the vector of control functions for a controlled quantum system, \hat{O} is a desired unitary transformation and \hat{U}_t is the time-evolution operator obtained from applying the control functions to the system in question.

Maximising such functionals is equivalent to minimising the euclidean distance between the operators \hat{O} and \hat{U}_t : $\|\hat{O} - \hat{U}_t\|^2 = \text{Tr}((\hat{O} - \hat{U}_t)^\dagger (\hat{O} - \hat{U}_t))$. This can be see by expanding out the right hand side and discarding terms that are constants as they have no effect on the optimisation.

3.2 Goal Operators

We need to choose specific unitary transformations as candidates for optimisation (the \hat{O} transform in eqn (11)). Permutation matrices are clearly unitary as they are orthogonal, and they are suitable initial candidates for goal operators.

As the $n \times n$ permutation matrices over \mathbb{C} are a faithful representation of the symmetric group of all permutations of n letters [7], there will be $n!$ such matrices. In the case of a system of N qubits, the time evolution operator is a $2^N \times 2^N$ matrix, and thus we consider all permutation matrices of the same size as potential goal operators.

There are $(2^N)!$ such matrices. For a $N = 2$ system, there are 24 such matrices. The identity can be excluded from further consideration as it can be trivially 'implemented' by any quantum system: after no time, nothing happens!

4 Numerical Method

4.1 Gradient Descent

Consider the problem of optimising (minimising) a function $f : \mathbb{R}^N \rightarrow \mathbb{R}$ (for some $N \in \mathbb{N}$). If one were performing gradient descent to minimise (assuming

Algorithm 1 Gradient descent pseudo-code

```
1:  $\mathbf{x} := \text{random\_vector}$ 
2: while  $f(\mathbf{x}) \leq \text{threshold}$  do
3:    $\mathbf{x}' := \mathbf{x} + \text{move\_size} * \text{random\_unit\_vector}$ 
4:    $\Delta := f(\mathbf{x}') - f(\mathbf{x})$ 
5:   if  $\Delta < 0$  then
6:      $\mathbf{x} := \mathbf{x}'$ 
7:   end if
8: end while
```

the existence of at least a single minimum) such an f , starting from a randomly chosen initial condition, then algorithm 1 would describe the method.

The ‘Grape’ (Gradient Ascent Pulse Engineering) algorithm for the discovery of control schemes has been well studied in the context of quantum computing and quantum optimal control in the presence of constrained control functions [9], [10]. It facilitates applying an iterative gradient ascent (or descent depending on the problems formulation, the two are equivalent) method to find control functions which maximise functionals of the form of eqn.(11).

The control ‘landscape’ for such functionals has also been studied [2], and has been found to potentially possess multiple optima. In the presence of local optima, gradient ascent methods of optimisation can become ‘trapped’. Hence one needs a more sophisticated search algorithm.

4.2 Simulated Annealing

Simulated annealing (SA) [3] is an alternative method to gradient descent for optimising a (real valued, sufficiently smooth) function of several (finitely many, real valued) variables that attempts to overcome the difficulty of local optima.

SA varies the gradient descent method by including a probabilistic acceptance of non-improving moves, in order to escape from local optima. In order to achieve this, a ‘cooling schedule’ is introduced via the introduction of a global ‘temperature’ variable that decreases as the system ‘cools’. When the system is ‘hot’ there is a relatively high chance of accepting a non-improving move, but after it has cooled significantly, this probability drops to zero. The probability of accepting a non-improving move is given by the Boltzmann distribution.

Algorithm 2 describes the method. Here T_0 is the initial temperature, and δT controls the cooling rate. These parameters are to be chosen according to the specific application; there is no known general principle for choosing the most effective values and experimentation is frequently needed to find effective values [3].

4.3 SA for constrained Fourier Series

In order to impose constraints, we augment standard SA with a rejection sampling method; moves are allowed only if the proposed new state does not violate the constraint.

Algorithm 2 Simulated Annealing pseudo-code

```
1:  $\mathbf{x} := \text{random\_vector}$ 
2:  $T := T_0$ 
3: while  $f(\mathbf{x}) \leq \text{threshold} \wedge 0 \leq T$  do
4:    $\mathbf{x}' := \mathbf{x} + \text{move\_size} * \text{random\_unit\_vector}$ 
5:    $\Delta := f(\mathbf{x}') - f(\mathbf{x})$ 
6:   if  $\Delta < 0 \vee \text{rand}(0, 1) \leq \exp(-\Delta/T)$  then
7:      $\mathbf{x} := \mathbf{x}'$ 
8:   end if
9:    $T := T - \delta T$ 
10: end while
```

Algorithm 3 Simulated Annealing for constrained Fourier series pseudo-code

```
1: repeat
2:    $\mathbf{G} := \text{random\_vector}$ 
3: until  $C(\mathbf{G})$ 
4:  $T := T_0$ 
5: while  $f(\mathbf{x}) \leq \text{threshold} \wedge 0 \leq T$  do
6:   repeat
7:      $\mathbf{G}' := \mathbf{G} + \text{move\_size} * \text{random\_unit\_vector}$ 
8:   until  $C(\mathbf{G}')$ 
9:    $\Delta := f(\mathbf{G}') - f(\mathbf{G})$ 
10:  if  $\Delta < 0 \vee \text{rand}(0, 1) \leq \exp(-\Delta/T)$  then
11:     $\mathbf{G} := \mathbf{G}'$ 
12:  end if
13:   $T := T - \delta T$ 
14: end while
```

Rejection sampling is implemented by repeating the generation of \mathbf{x}' in the SA algorithm 2 (line 4) until the constraint is satisfied.

Let \mathbf{G} be the relevant vector of Fourier coefficients $\{a_{k,m}, b_{k,m}\}$. Let $C()$ be the Boolean-valued constraint on the Fourier coefficients. Then algorithm 3 describes our rejection sampling constrained SA method.

We use constrained SA to search for the Fourier coefficients for each of the control functions. We impose the following fidelity constraint:

$$\phi = \int_0^\tau g_k^2(t) dt = \frac{1}{\tau} \sum_{n=0}^M (a_n^2 + b_n^2) \leq \kappa^2 \quad (12)$$

and we arbitrarily choose $\kappa = 1$ for convenience.

4.4 The Fitness Function

We analyse the effectiveness of constrained SA in the discovery of time optimal control functions that result in a spin-chain systems implementing a permutation of set of (orthonormal) basis vectors. This can be achieved by considering

functionals of the form:

$$F[\mathbf{g}, \tau] = \Re \text{Tr}(\hat{P}^\dagger \hat{U}_\tau) - \tau^2 \quad (13)$$

where P is a permutation matrix (see § 3.2). Here we are maximising F ; the τ^2 term is included to ‘punish’ slow implementations and reward faster ones.

In order to find time optimal solutions, we vary the Fourier coefficients of the control functions as described in algorithm 3; we also vary τ (the time the spin chain’s dynamics is evolved for in order to calculate the fitness function) by a random amount between -0.001 and 0.001 with each iteration of SA. This is performed at the same step of the algorithm as varying the Fourier coefficients (algorithm 3, line 7). A similar method of rejection sampling is used to prevent τ becoming negative.

The simulation was performed using a standard geometric integrator build into the Matlab symbolic math package.

In the SA process, the termination criterion was chosen so that the algorithm would terminate only if a fitness of $F \geq 0.7$ was achieved (eqn.(13)), and a fidelity of $\phi \geq 0.92$ was achieved (eqn.(12)), or 500 iterations had been performed.

5 Results

We present the results for six specific permutations (§3.2) in table 1. These demonstrate all the behaviours exhibited by the SA algorithm during our experiments.

Throughout our investigation we choose the Fourier band limit (eqn.(2)) to be $M = 5$.

5.1 Two qubits, each with two orthogonal control fields

In the two control field case ($h_n \neq 0$), we found the algorithm to exhibit a variety of behaviours with the parameters chosen. We saw three types of run:

1. The matrices which achieved a fidelity of greater than 0.92 converged quickly (in about 200 iterations). The reduction of the gate implementation time as the SA proceeded did not seem to limit the progress towards a high fidelity control scheme. This suggests that the algorithm did not find solutions approaching the time optimal ones, as no trade off between fidelity and time optimality was observed. An example graph of the progress of fidelity during such a run of SA can be seen in fig.1, and for the progress of implementation time in fig.2.
2. Some of the matrices which did not achieve a fidelity of greater than 0.92 seemed to stagnate in their progress to increasing fidelity as the implementation time reached a critical low point. These ‘stagnation points’ occur at a fidelity of around 0.5 – 0.6; after this little progress was made before the algorithm timed out. This suggests that a point was reached where time optimality and fidelity were in direct conflict. An example graph of the progress

P	1 control field (g)		2 control fields (g, h)	
	max fidelity ϕ	min time τ	max fidelity ϕ	min time τ
$\begin{pmatrix} 1 & 0 & 0 & 0 \\ 0 & 1 & 0 & 0 \\ 0 & 0 & 0 & 1 \\ 0 & 0 & 1 & 0 \end{pmatrix}$	0.057	0.499	0.540	0.456
$\begin{pmatrix} 1 & 0 & 0 & 0 \\ 0 & 0 & 1 & 0 \\ 0 & 1 & 0 & 0 \\ 0 & 0 & 0 & 1 \end{pmatrix}$	0.563	0.564	0.553	0.486
$\begin{pmatrix} 0 & 1 & 0 & 0 \\ 1 & 0 & 0 & 0 \\ 0 & 0 & 0 & 1 \\ 0 & 0 & 1 & 0 \end{pmatrix}$	–	–	0.92	0.679
$\begin{pmatrix} 0 & 1 & 0 & 0 \\ 0 & 0 & 0 & 1 \\ 0 & 0 & 1 & 0 \\ 1 & 0 & 0 & 0 \end{pmatrix}$	–	–	0.587	0.592
$\begin{pmatrix} 0 & 0 & 1 & 0 \\ 0 & 0 & 0 & 1 \\ 1 & 0 & 0 & 0 \\ 0 & 1 & 0 & 0 \end{pmatrix}$	–	–	0.92	0.693
$\begin{pmatrix} 0 & 0 & 0 & 1 \\ 0 & 0 & 1 & 0 \\ 0 & 1 & 0 & 0 \\ 1 & 0 & 0 & 0 \end{pmatrix}$	0.078	0.854	0.92	0.693

Table 1. 2-qubit results with one and two control fields per qubit

of fidelity during such a run of SA can be seen in fig.3; and for the progress of implementation time in fig.4.

- Other matrices which did not achieve a fidelity of greater than 0.92 seemed to be progressing but simply too slowly to achieve a suitable result before the 500 iteration timeout. Further work will include extending the timeout, with better “stagnation” detection.

This collection of behaviours suggest that a modification to the fitness function is needed. High fidelity is essential for the implementation of quantum gates, and should be given a higher precedence over time optimality. A fitness function that rewards both speed and high fidelity, but without allowing time optimality to compromise fidelity, is needed. The search for such a fitness function will also be the basis for further work.

Some of the optima found in the two control fields per qubit cases are close to the global ones (in terms of the fidelity alone, not time optimality); in future work the control schemes found with the SA method will be compared explicitly to theoretical optima for time optimality. The cases this applies to are those with two control fields per qubit which reached a fidelity of 0.92 or greater.

The results attempt to provide a minimum implementation time, given the energy constraint or at least to demonstrate that the SA method is capable or providing such information about a system. This will allow us to investigate the tightness of speed limit bounds for specific quantum operations.

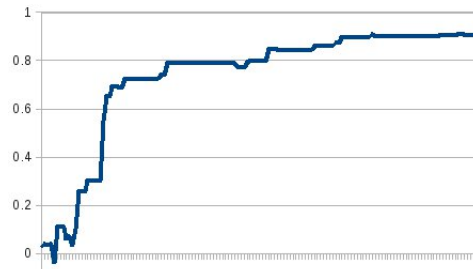


Fig. 1. Progress of fidelity ϕ in a two field case where convergence occurred

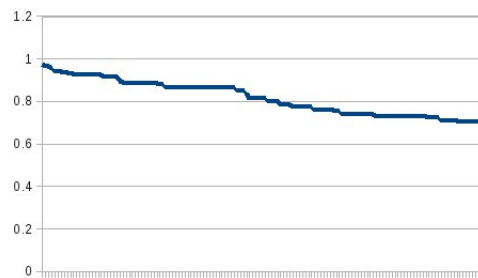


Fig. 2. Progress of implementation time τ in a two field case where fidelity convergence towards 1 occurred

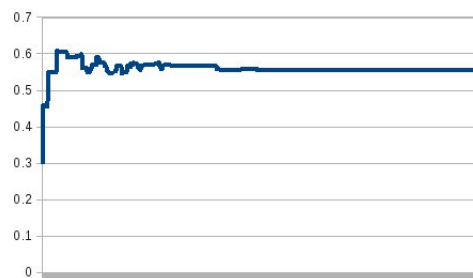


Fig. 3. Progress of fidelity ϕ in a two field case where stagnation occurred

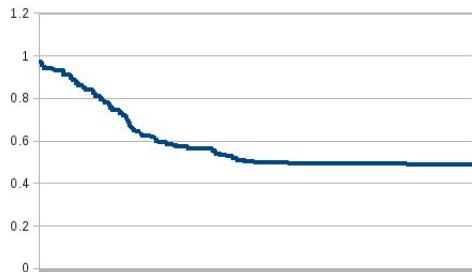


Fig. 4. Progress of implementation time τ in a two field case where stagnation occurred

5.2 Two qubits, each with a single control field

In the case of two qubits each with a single control field, the results were found to be less promising, and no fast, high fidelity schemes were found. What was observed was either the SA converged to a solution with fidelity far from one, or it failed to converge, with fidelity and implementation times remaining close to their initial values until timeout (cases where this happened are marked – in the results table 1). This may be because this system in question is simply not ‘controllable’, and cannot implement the gate required, with the single field constrained control functions of the form used. However, it is difficult to tell this situation apart from a failure of the algorithm due to bad choice of parameters.

In the cases where convergence occurred, there was a similar pattern of search behaviours as in the two control field case. Either a point where time optimality was hindering progress towards a higher fidelity solution was reached and progress stagnated, or fidelity began to converge (frequently at about 0.5) as the implementation continued to decrease the time, unhampered by the convergence of fidelity. In the later cases the algorithm timed out, and it is apparent that a higher timeout value is needed to probe this scenario further.

6 Conclusions and Further Work

We have introduced a form of SA, constrained SA, suitable for searching for optimal solutions under constraints. We have found that this constrained SA shows potential as an effective method for discovering optimal control schemes for Heisenberg spin chains subject to constrained control functions. We have also found that it opens many directions for future work. The approach is readily extensible to other quantum computational systems, and to other constraints and could be a good tool for studying constrained, quantum time optimal control.

The numerical results additionally provide information on the implementability of specified gates using particular control schemes.

Next steps include:

1. a direct comparison of constrained SA to GRAPE

2. a comparison of the numerically discovered implementation time of optimal control schemes to theoretical speed limit bounds
3. an investigation of the role of the Fourier band limit M on the time optimality of control schemes discovered by constrained SA
4. an investigation of other relevant physical constraints
5. design of a better fitness function for SA so that fidelity is never compromised.

Acknowledgments

We thank Simon Poulding for many helpful discussions. Russell is supported by an EPSRC DTA grant.

References

1. C. Altafini and F. Ticozzi. Modeling and Control of Quantum Systems: An Introduction. *IEEE Transactions on Automatic Control*, 57:1898–1917, 2012.
2. Michael Hsieh and Herschel Rabitz. Optimal control landscape for the generation of unitary transformations. *Phys. Rev. A*, 77:042306, Apr 2008.
3. P. J. M. Laarhoven and E. H. Aarts. *Simulated Annealing: Theory and Applications*. Springer, 1987.
4. Seth Lloyd. Ultimate physical limits to computation. *Nature*, 406(6799):1047–1054, 1999.
5. Norman Margolus and Lev B. Levitin. The maximum speed of dynamical evolution. *Physica*, D120:188–195, 1998.
6. P. Mohn. *Magnetism in the Solid State: An Introduction*. Springer, 2003.
7. Gilbert de B. Robinson. *Representation theory of the symmetric group*. Edinburgh University Press, 1961.
8. Benjamin Russell and Susan Stepney. Geometric methods for analysing quantum speed limits: time-dependent controlled quantum systems with constrained control functions. In *Unconventional Computation and Natural Computation 2013, Milan, Italy, July, 2013*, LNCS. Springer, 2013. (this proceedings).
9. Thomas Schulte-Herbruggen. Controlling quanta under constraints. 2007. (presentation, <http://www.impan.pl/BC/Arch/2007/CCQ/Schulte-Herbrueggen.pdf>).
10. Thomas Schulte-Herbruggen. Quantum compilation by optimal control of open systems. 2007. (presentation, http://www.physik.uni-siegen.de/quantenoptik/events/marialaach07/schulte-herbrueggen_marialaach07.pdf).
11. J. Werschnik and E. K. U. Gross. Quantum Optimal Control Theory. *ArXiv e-prints*, July 2007. arXiv:0707.1883 [quant-ph].
12. M. Zwierz. Comment on “Geometric derivation of the quantum speed limit”. *Physical Review A*, 86:016101, 2012.